Electric dipole strength of the Borromean double halo nucleus ^{11}Li using proton inelastic scattering

J.M. López-González, Y. Ayyad, D. Bazin, J.C. Zamora, S.M. Ali, C. Ardelean, A. Barioni, F. Barranco, S. Beceiro-Novo, C. Benetti, C. Cabo, J. Chen, W. Dominik, M. Gai, U. Garg, S. Giraud, M.N. Harakeh, B.P. Kay, M. Kuich, J.A. Lay, C. Maher, G.W. McCann, A.J. Mitchell, W. Mittig, S. Noji, B. Olaizola, S. Painter, N.D. Pathirana, J. Pereira, G. Potel, Z. Rahman, D. Ramirez, Z. Serikow, D.K. Sharp, E. Vigezzi, B. Votaw, B. Wagner and R.G.T. Zegers

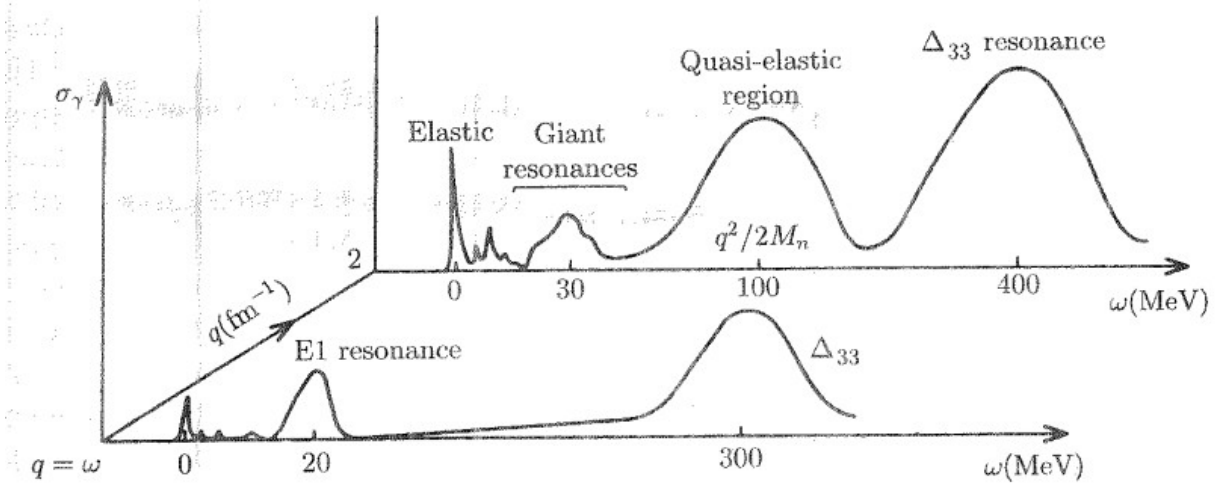
06/11/2026

Rede CIGUS
Centros de investigación do Sistema Universitario de Galicia
Cofinanciado por la Unión Europea
Fondos Europeos
Xacobeo 2027

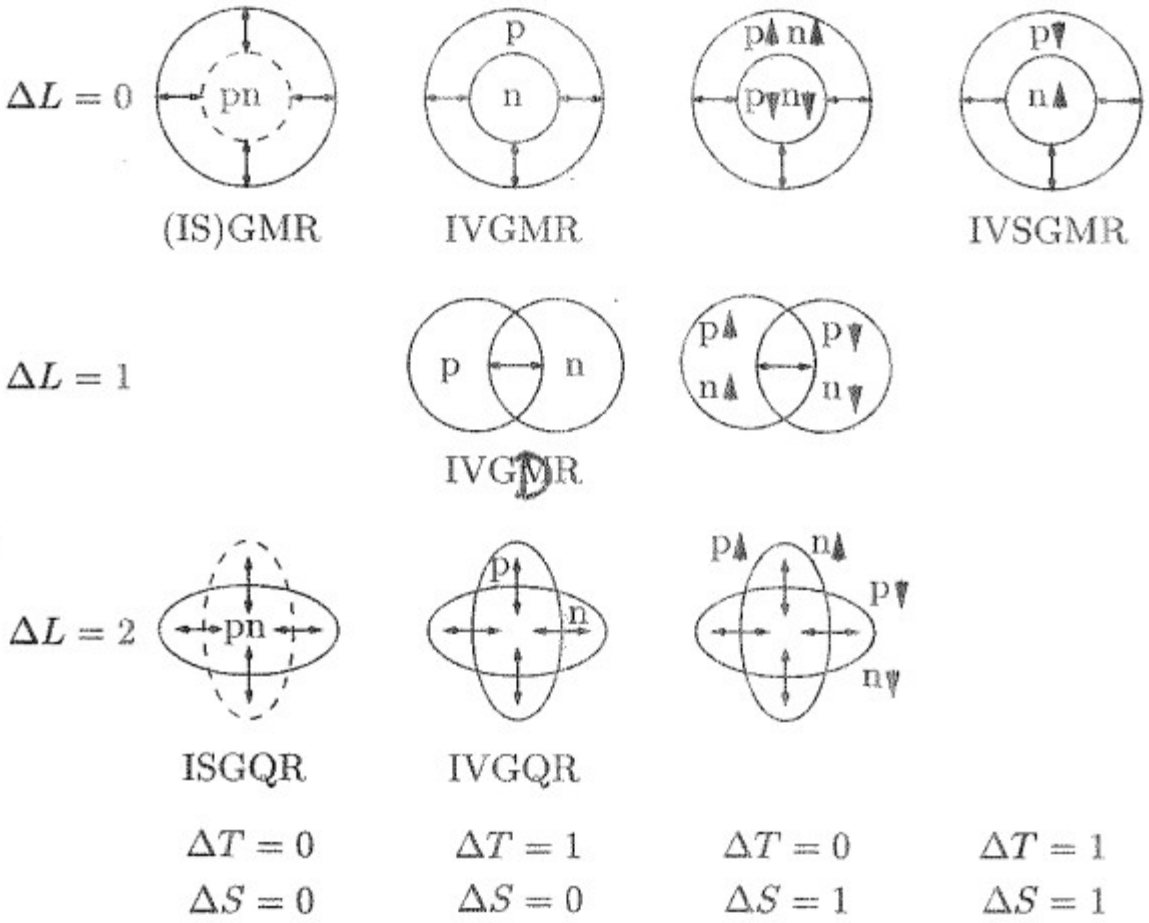
Outline

1. Motivation and physics case.
2. Experimental setup.
3. Analysis.
4. Preliminary results.
5. Summary.

Motivation: Giant Resonances



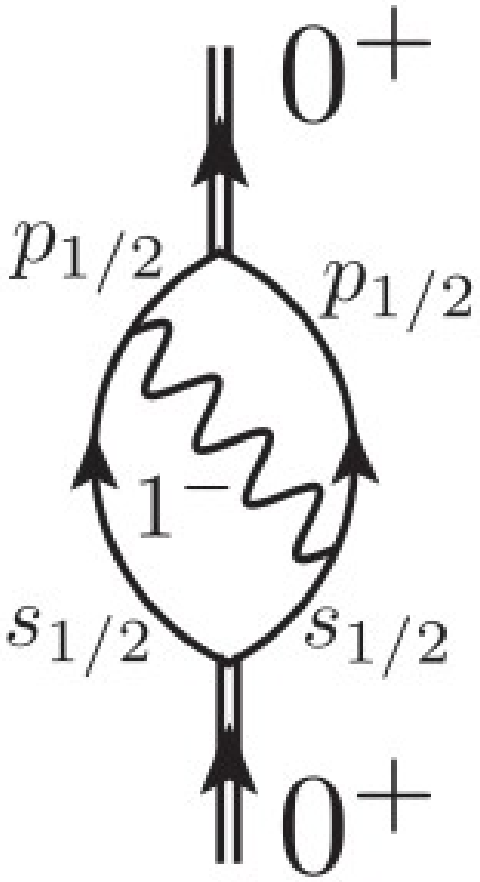
$$\sum_n (E_n - E_0) B(\mathrm{E1}, 0 \to n) = 14.8 \frac{NZ}{A} (1 + \kappa)\, e^2\, \mathrm{fm}^2\, \mathrm{MeV}$$

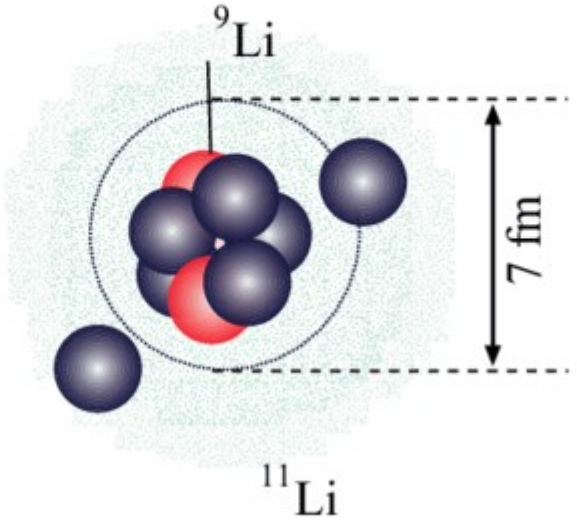


Source: M.N. Harakeh and A. van der Woude. Giant Resonances.

Physics case: Electric dipole response of ^{11}Li

While ^{10}Li is unbound, ^{11}Li is bound due to the pairing interaction of the 2 neutrons in its halo, which form a **Cooper pair**, with a 2-neutron separation energy of just 396 keV.

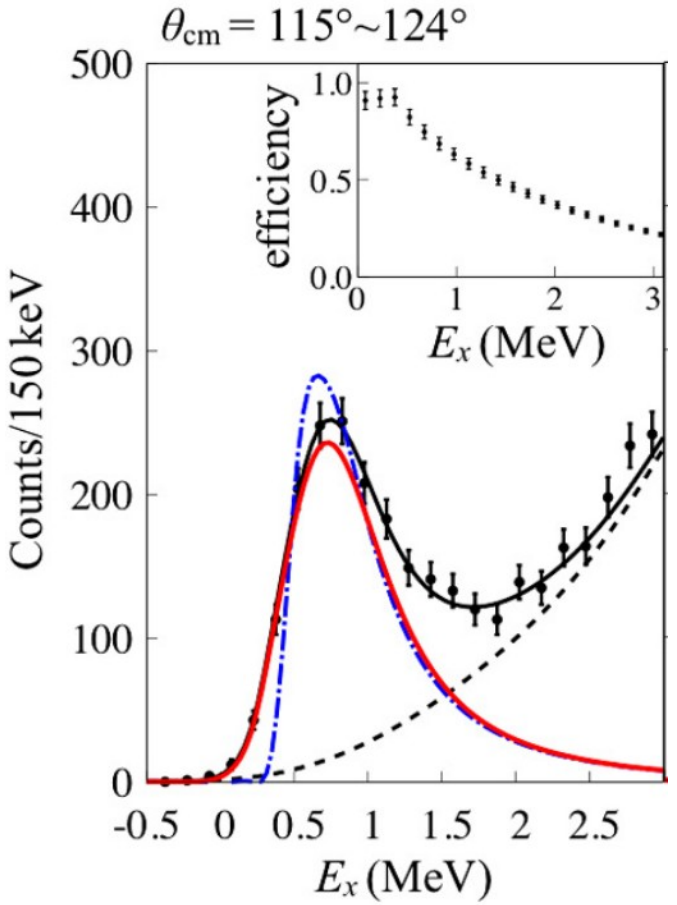




However, the full E1 response is needed in order to determine quantities like the nuclear **electric dipole polarizability**.

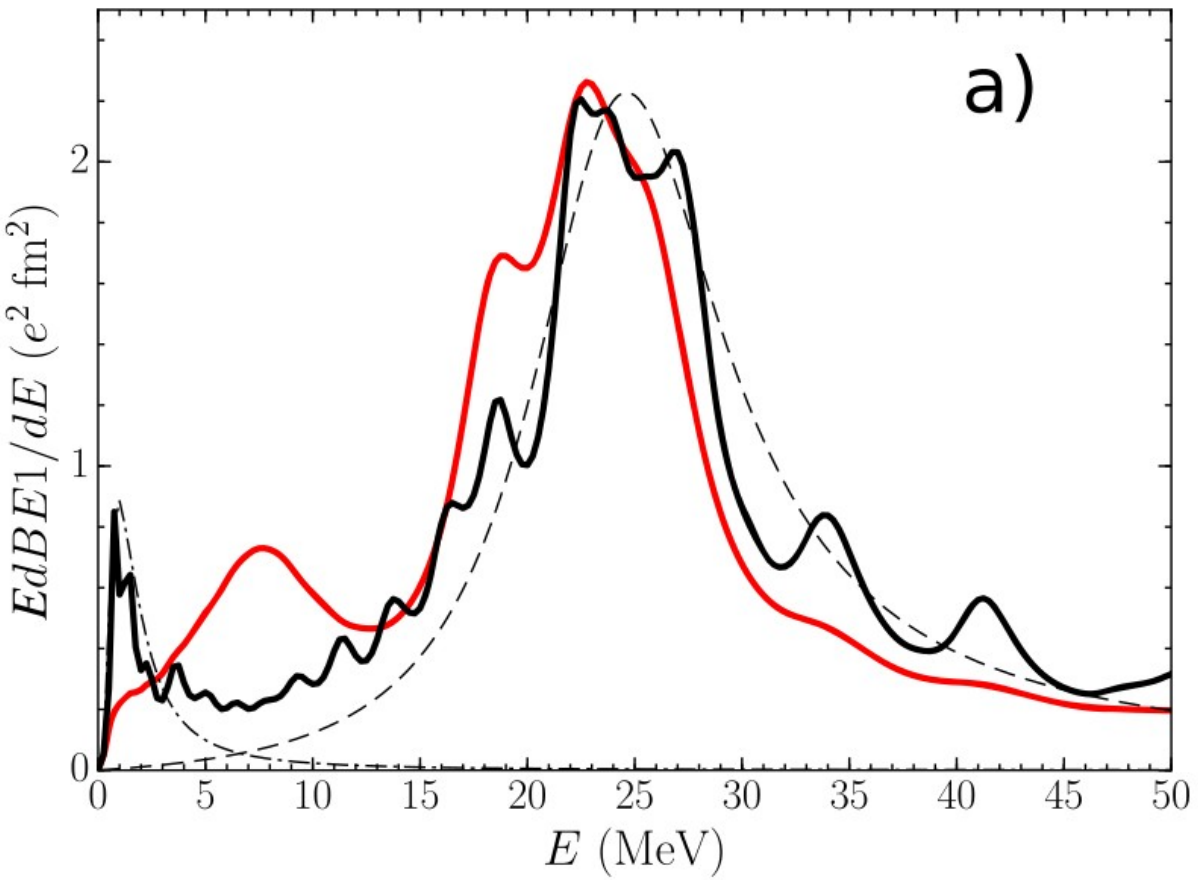
$$\alpha_D = \frac{8\pi}{9} \int \frac{dB\,(E1)}{\omega}$$

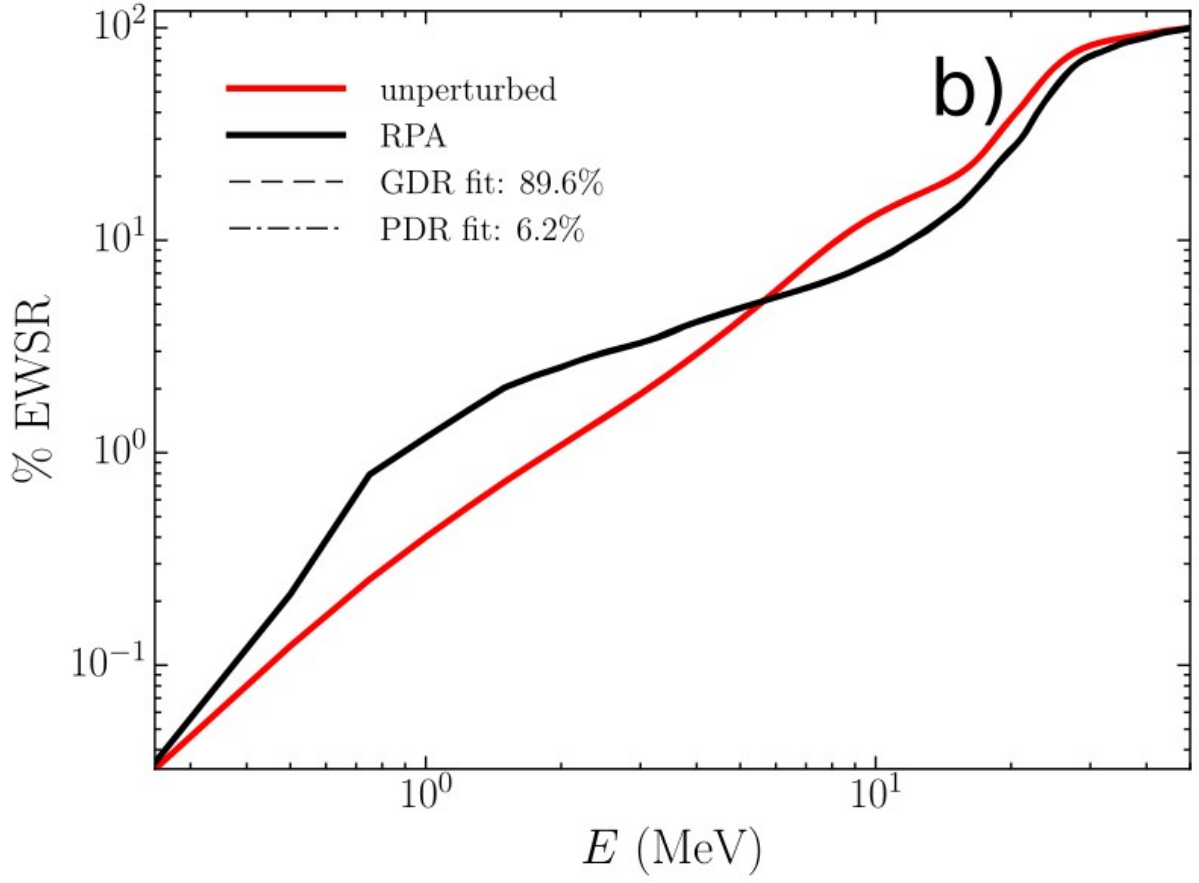
Only a very small amount of the total E1 response of ^{11}Li has been measured so far, which corresponds to its **Pygmy dipole resonance**.



Sources:
1. B. Jonson, Phys. Rep. 389, 1 (2004)
2. R.A. Broglia et al., Physica Scripta Volume 94, Number 11 (2019)
3. J. Tanaka et al Phys. Lett. B 774 (2017) 268–272

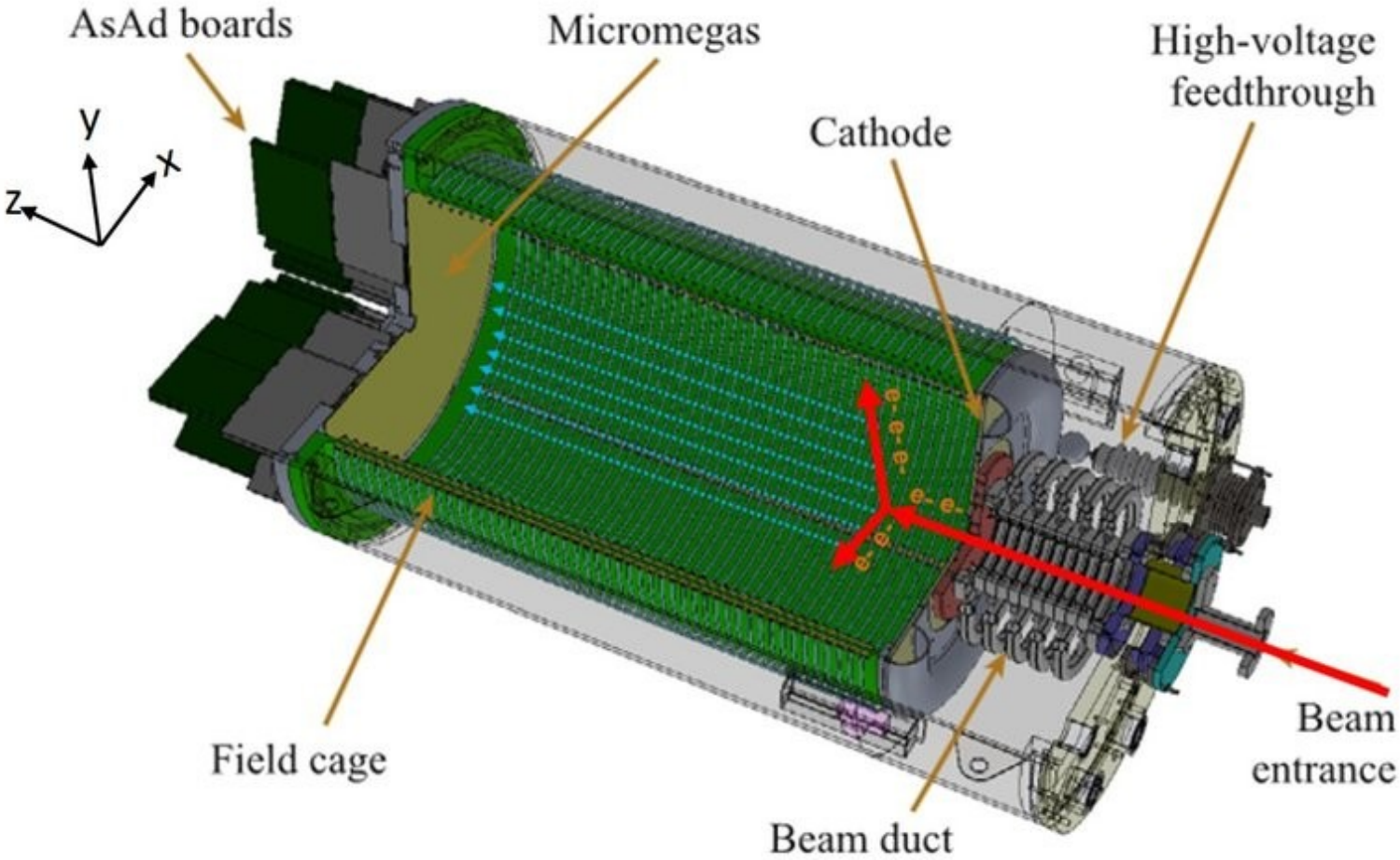
Theory prediction of the full E1 response of ^{11}Li





Source: R. A. Broglia et al 2019 Phys. Scr. 94 114002

Experimental details: The



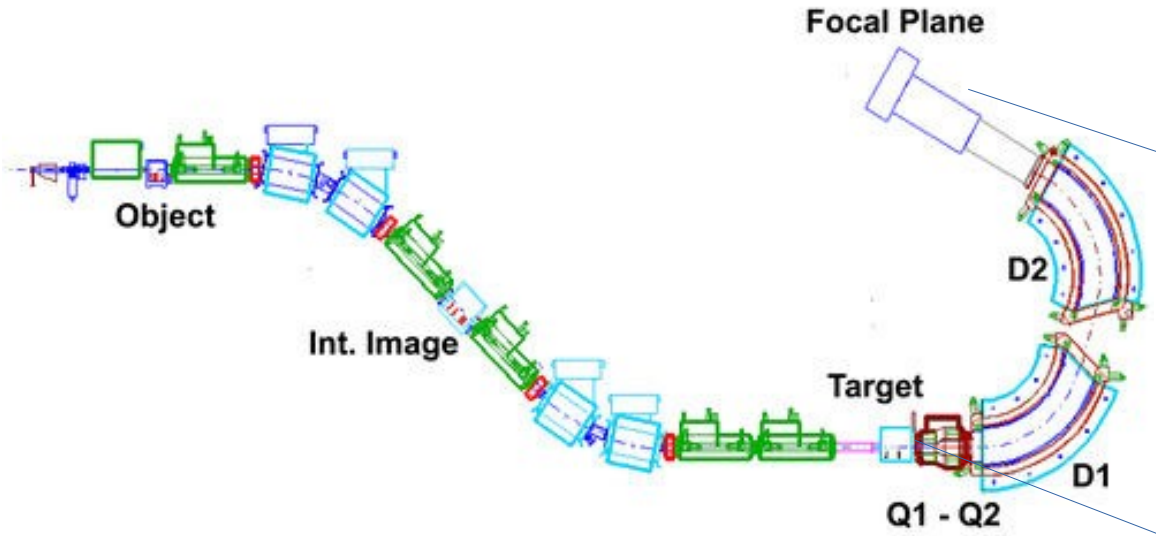
Used as the **active target** for the experiment, with 2 settings:
A) Pure H_2@600Torr
B) 90% H_2 + 10% CF_4@700Torr

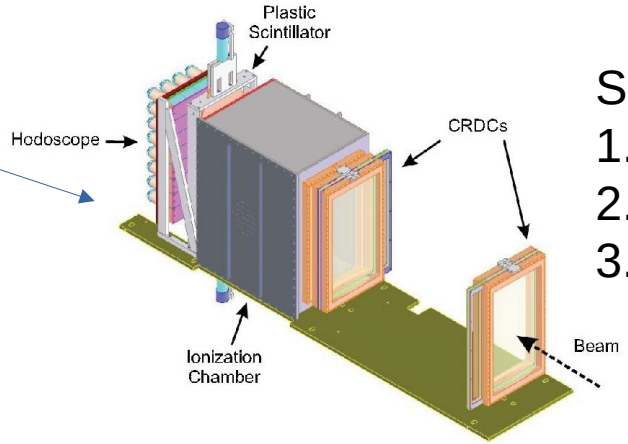
Also used to **track the scattered proton**, allowing us to obtain its kinetic energy and its scattering angle.

By using doing a **missing mass 2-body kinematics calculation**, the excitation energy and CM scattering angle can be determined.

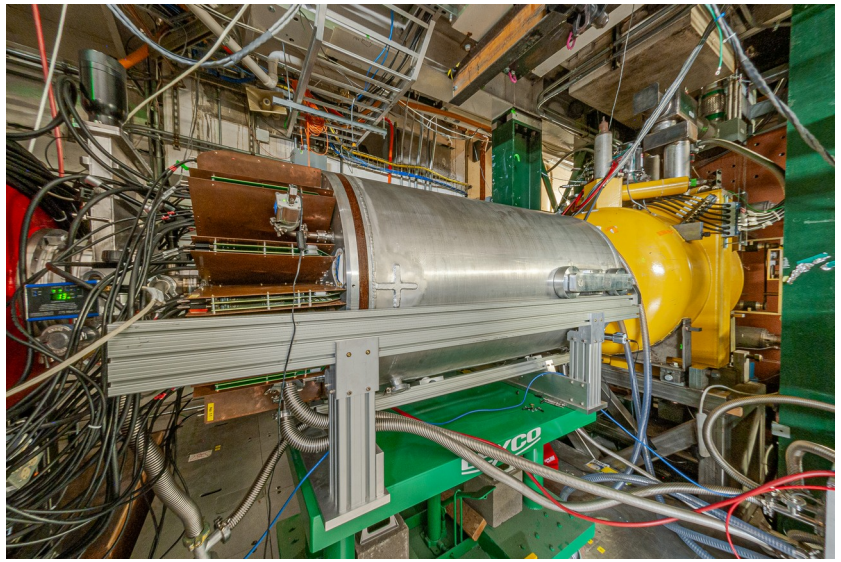
Source: J.S. Randhawa et al. Nuclear Instruments and Methods in Physics Research Section A: Accelerators, Spectrometers, Detectors and Associated Equipment, Volume 948, 21 December 2019, 162830

Experimental details: The S800 spectrograph





S800 detectors are used for:
1. DAQ trigger.
2. Beam PID.
3. Decay product PID.



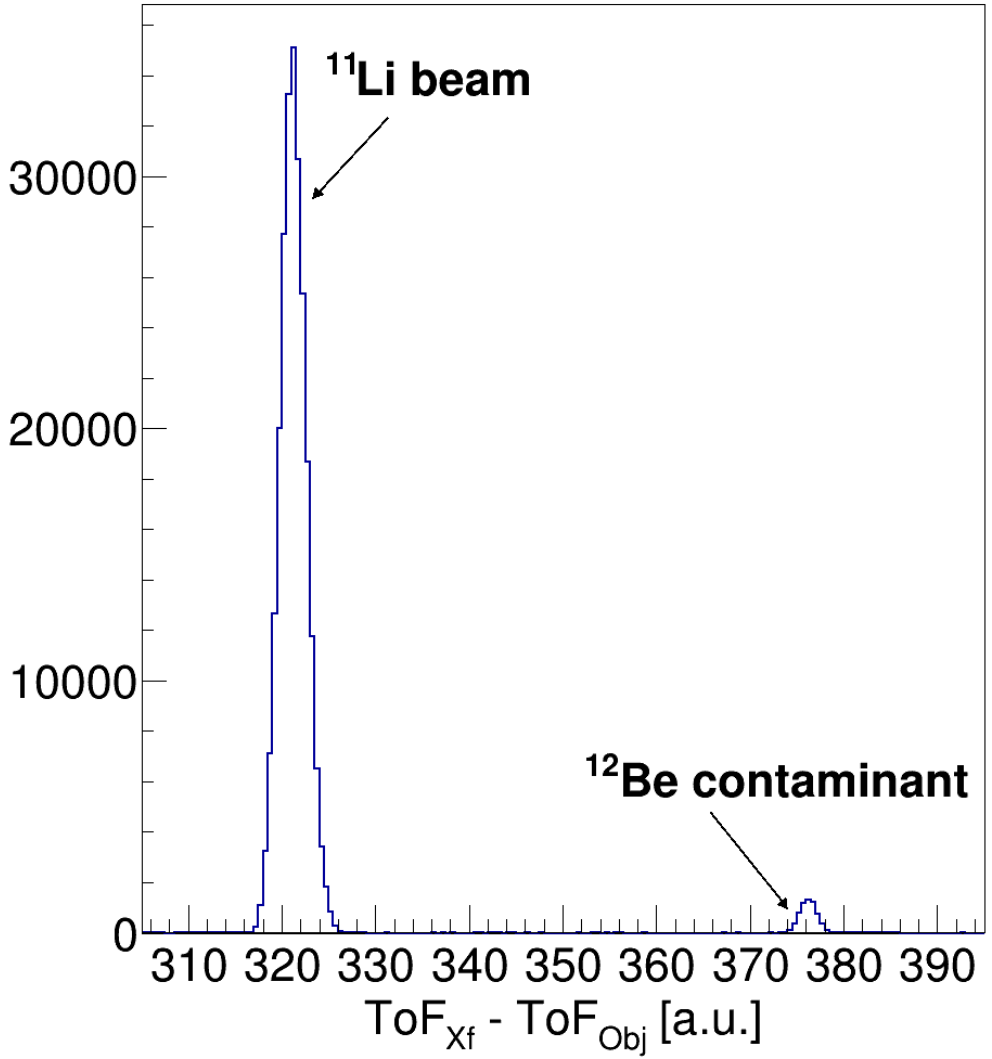
~10^4 pps ^{11}Li beam at 53.36 MeV/u, with a small ^{12}Be contaminant.

Reaction to study: $^{11}Li + p \rightarrow {}^{11}Li^* + p' \rightarrow X + p'$

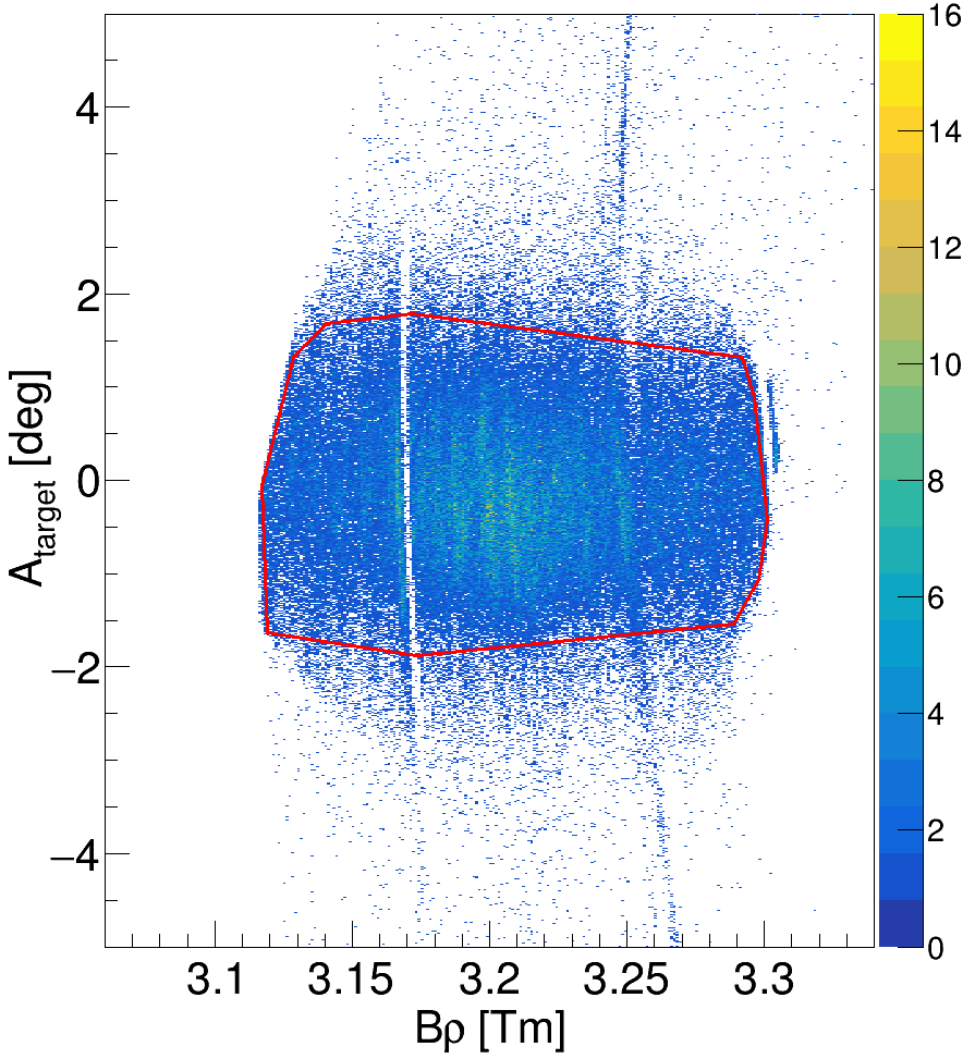
- $X = {}^{9}Li + 2n$
- $X = {}^{7}Li + 4n$
- $X = {}^{8}Li + 3n$
- $X = {}^{4}He + 4n + t$

Sources: 1. https://wikihost.frib.msu.edu/S800Doc/doku.php
2. https://people.frib.msu.edu/~noji/pictures

S800 Analysis: Beam PID and S800 acceptance window

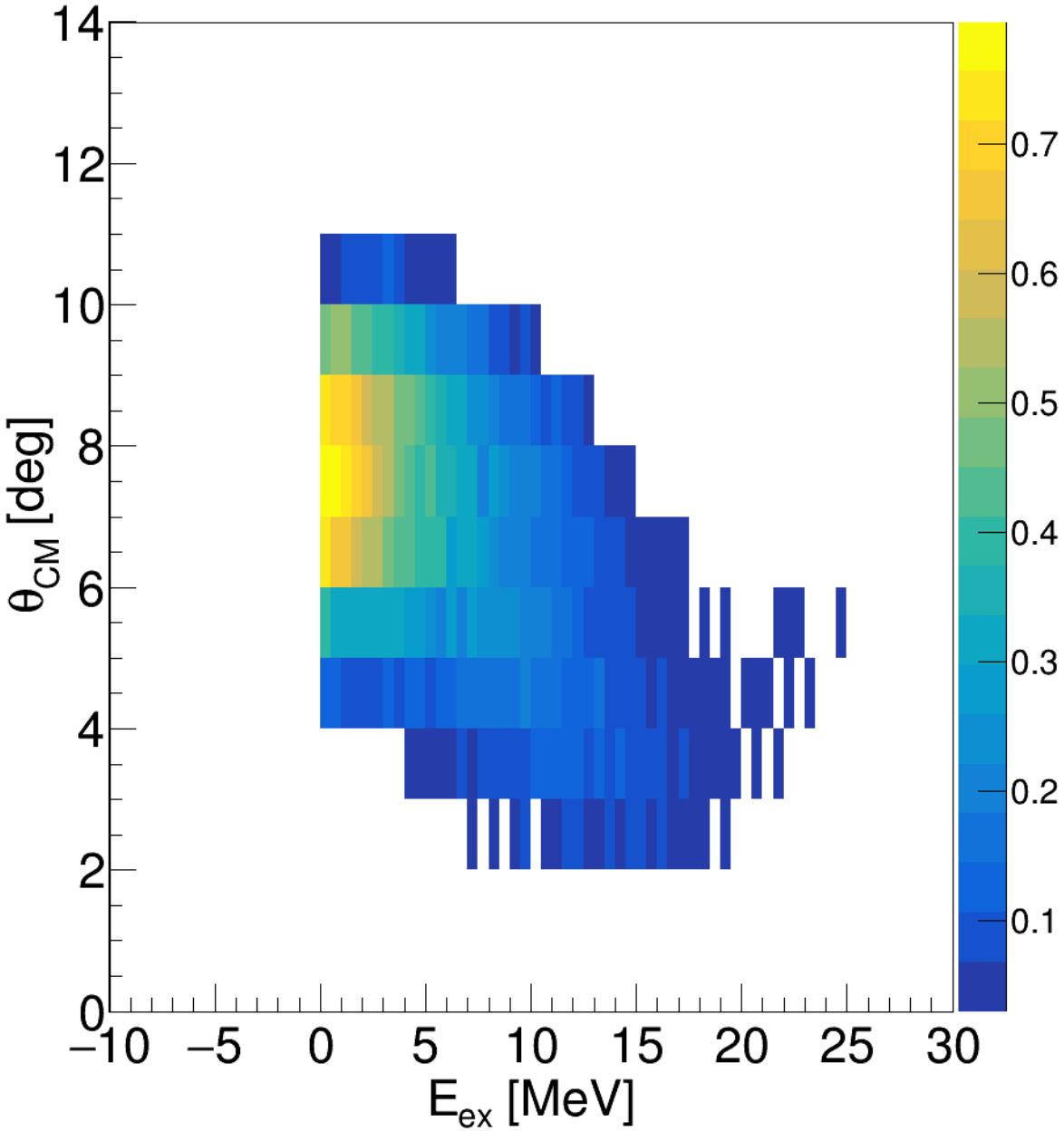


Beam PID is done measuring the ToF between the S800 Object station and the A1900 intermediate focal plane.



From positions and angles measured at the focal plane, the dispersive angle and magnetic rigidity of the decay products can be obtained at the target position using the **inverse map method**, which ultimately gives us the **acceptance window**.

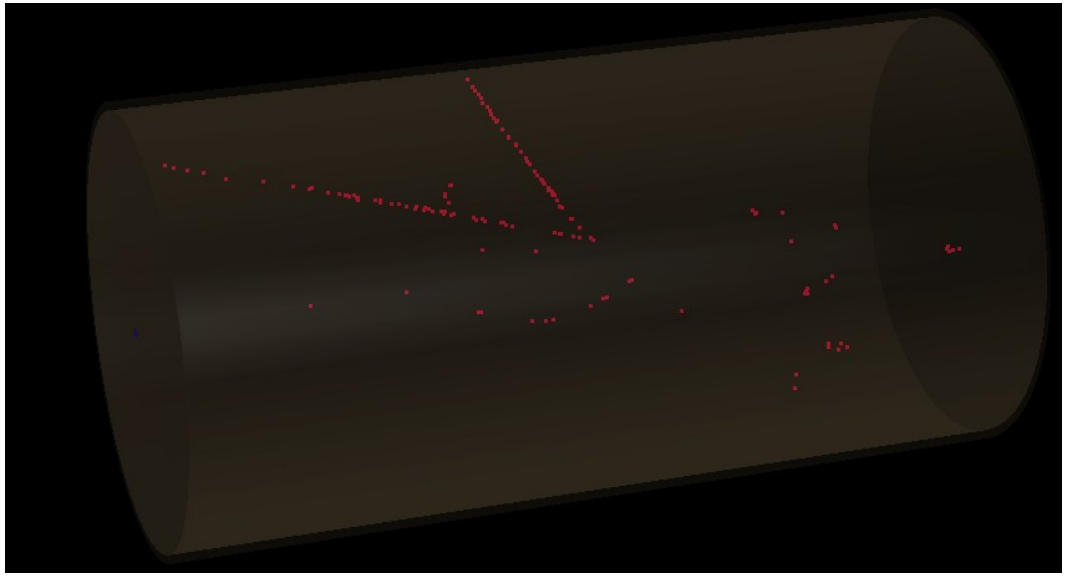
Simulation: Total setup efficiency



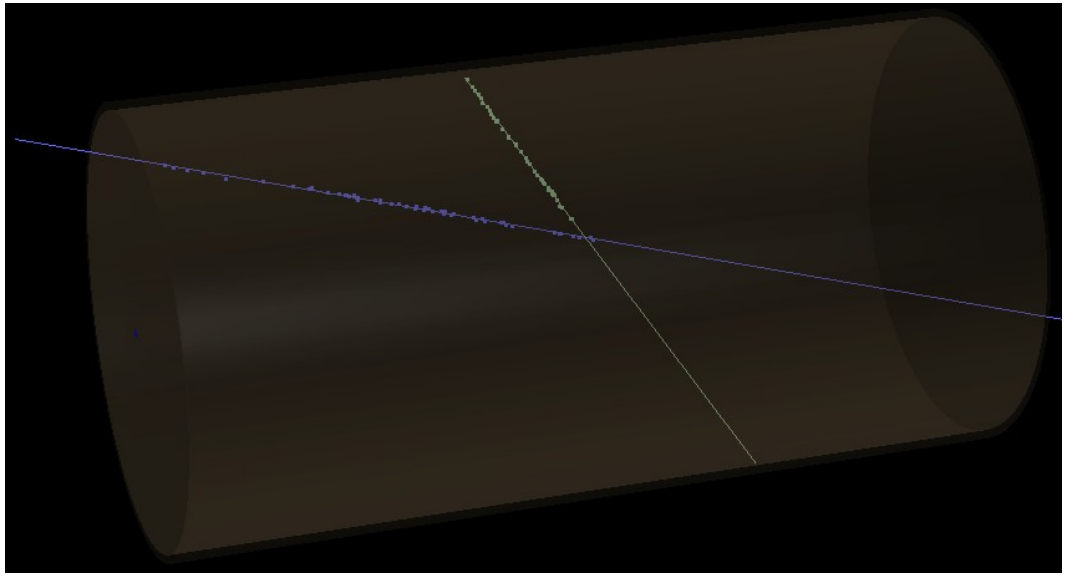
The **total efficiency** of the setup is given by **4 conditions**:

1. The scattered proton must exit the beam region.
2. The scattered proton must not punch-through.
3. The decay product must reach the exit hole of the AT-TPC that connects with the S800. For higher excitation energies, the maximum decay angle increases, so the efficiency becomes smaller.
4. The decay product must be inside the magnetic rigidity acceptance window.

AT-TPC Analysis: RANdom SAmple Consensus (RANSAC)



RANSAC



After reconstruction of the cloud of hits of the event, a RANSAC algorithm is used in order to find **straight tracks**.

Additionally, the intersection between the tracks and the Z axis provides us with the **reaction vertex**. This allows us to correct for the **energy loss of the beam particle** using **CATIMA**.

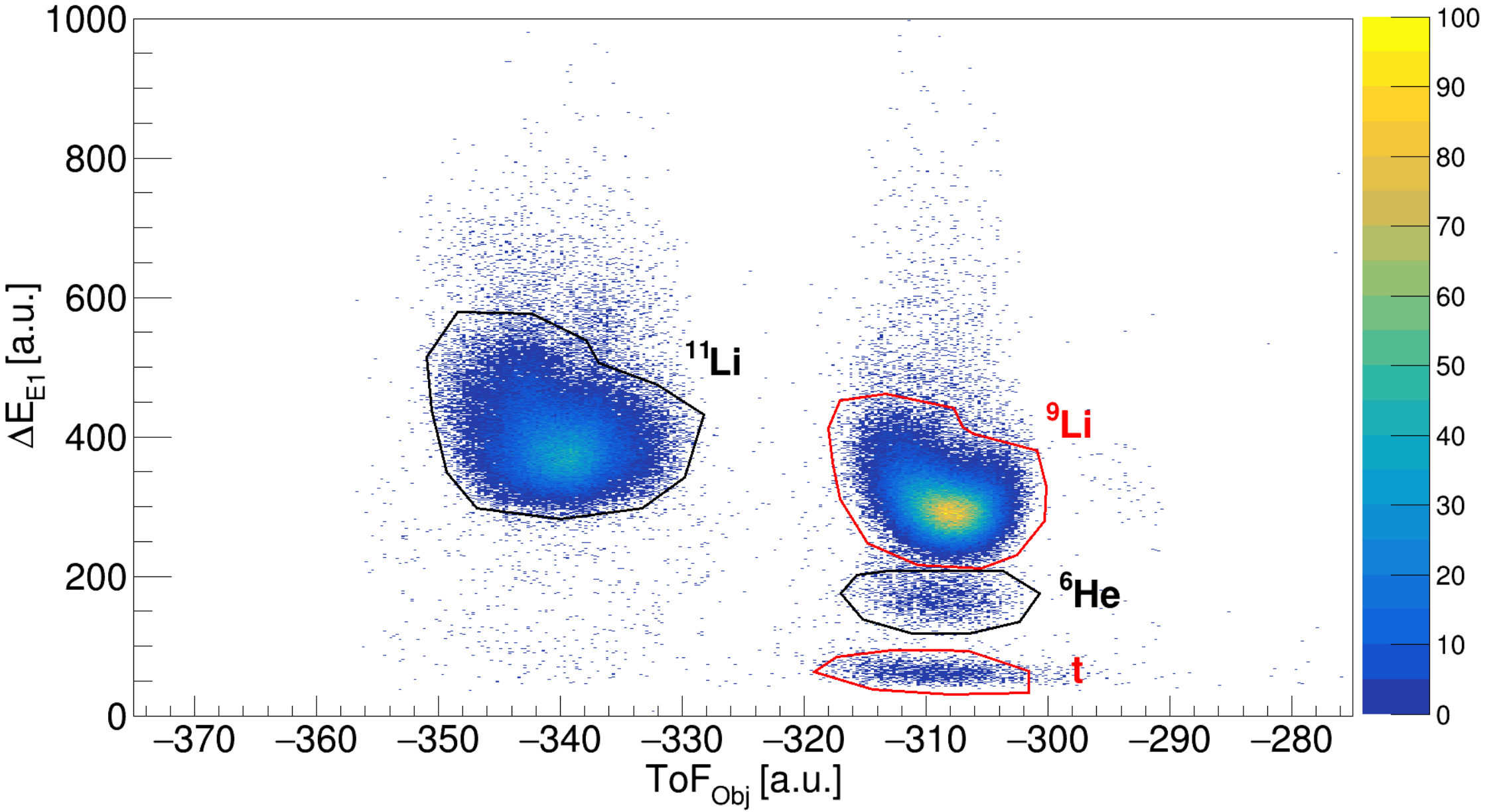
The distance from the last point of each track to the reaction vertex is the **range** of the particle, which can then be translated into **kinetic energy** using SRIM energy loss tables. The **scattering angle** is then obtained by the RANSAC fit line.

Depending on the decay channel of the S800 setting, **only events with 1 or 2 tracks per vertex are accepted**.

Preliminary results!

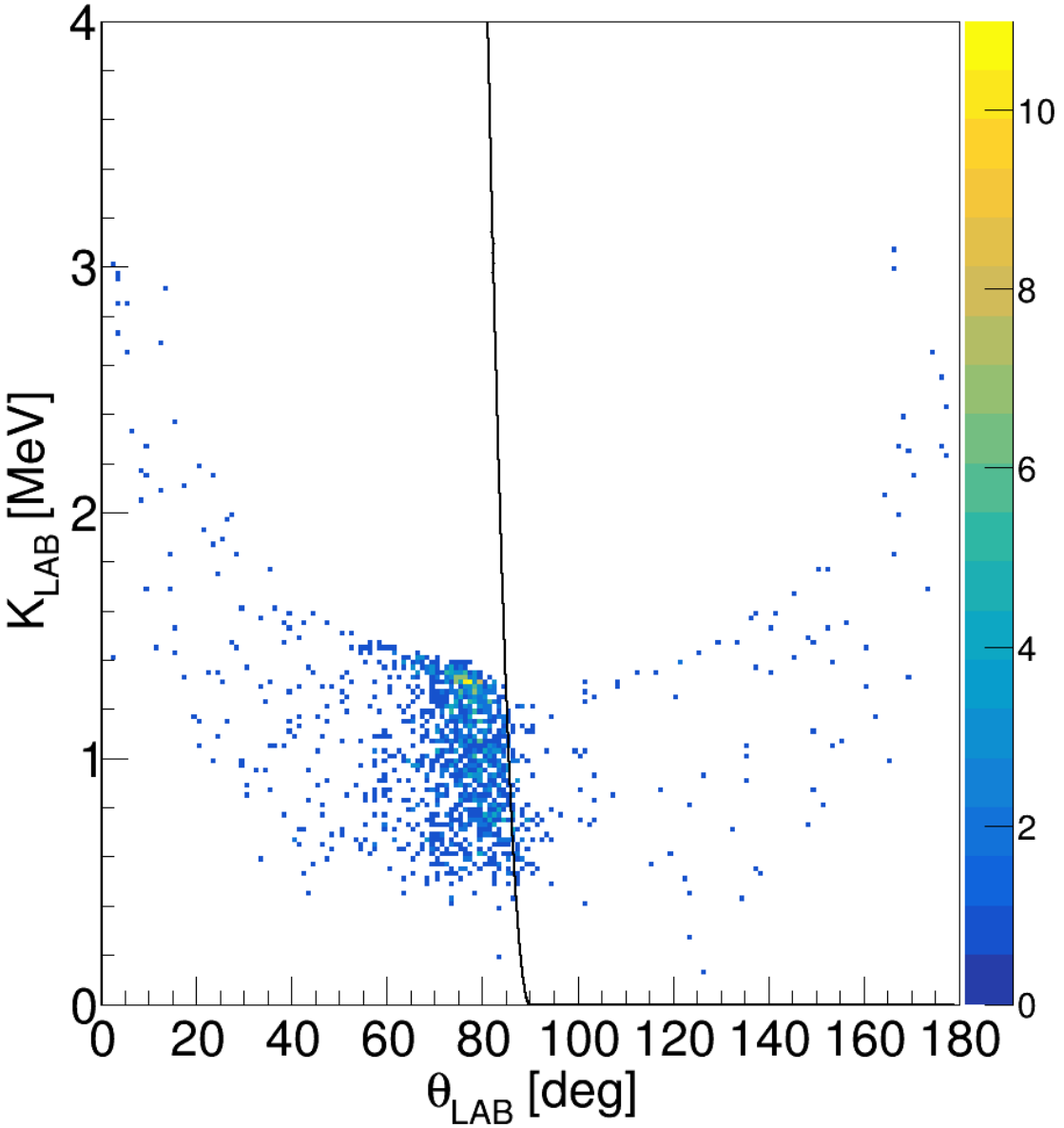
- S800 centered on ^{9}Li with H_2@600Torr
- S800 centered on ^{8}Li with H_2@600Torr
- S800 centered on ^{7}Li with H_2@600Torr
- S800 centered on ^{4}He with H_2+CF_4@700Torr

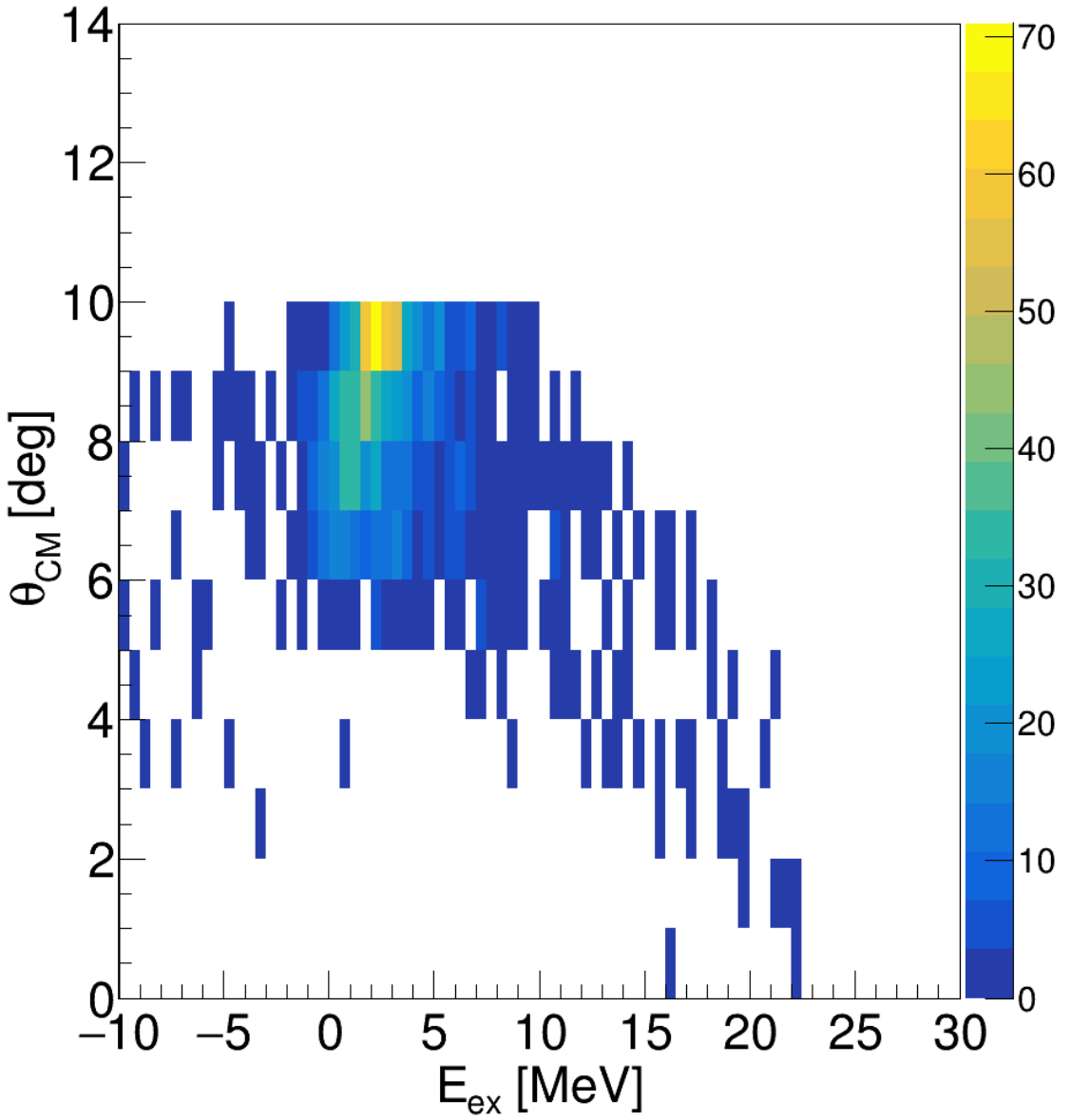
S800 centered on ^{9}Li with H_2@600Torr: Decay PID



$^{11}Li + p \rightarrow {}^{9}Li + 2n + p'$

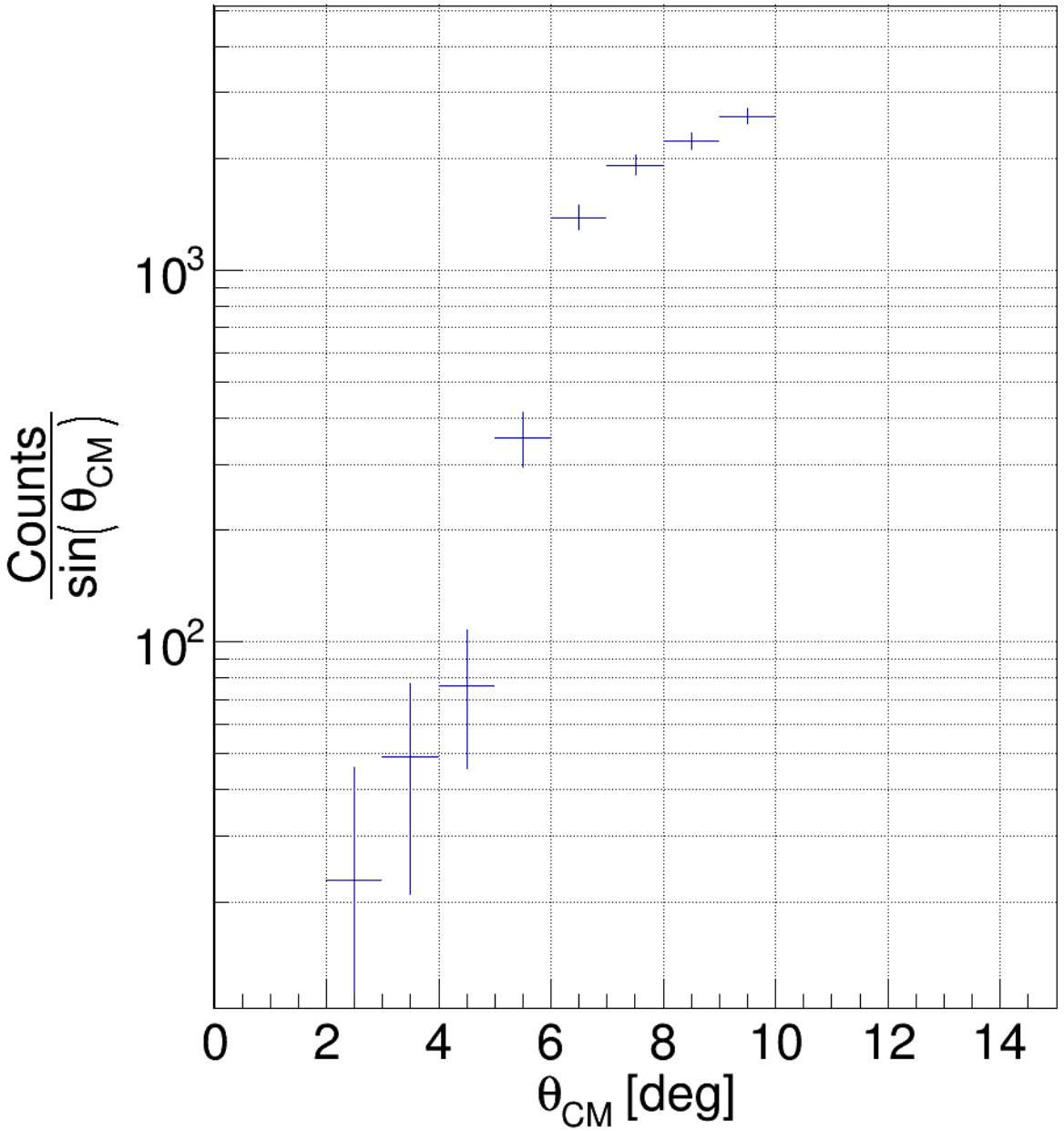
PRELIMINARY!

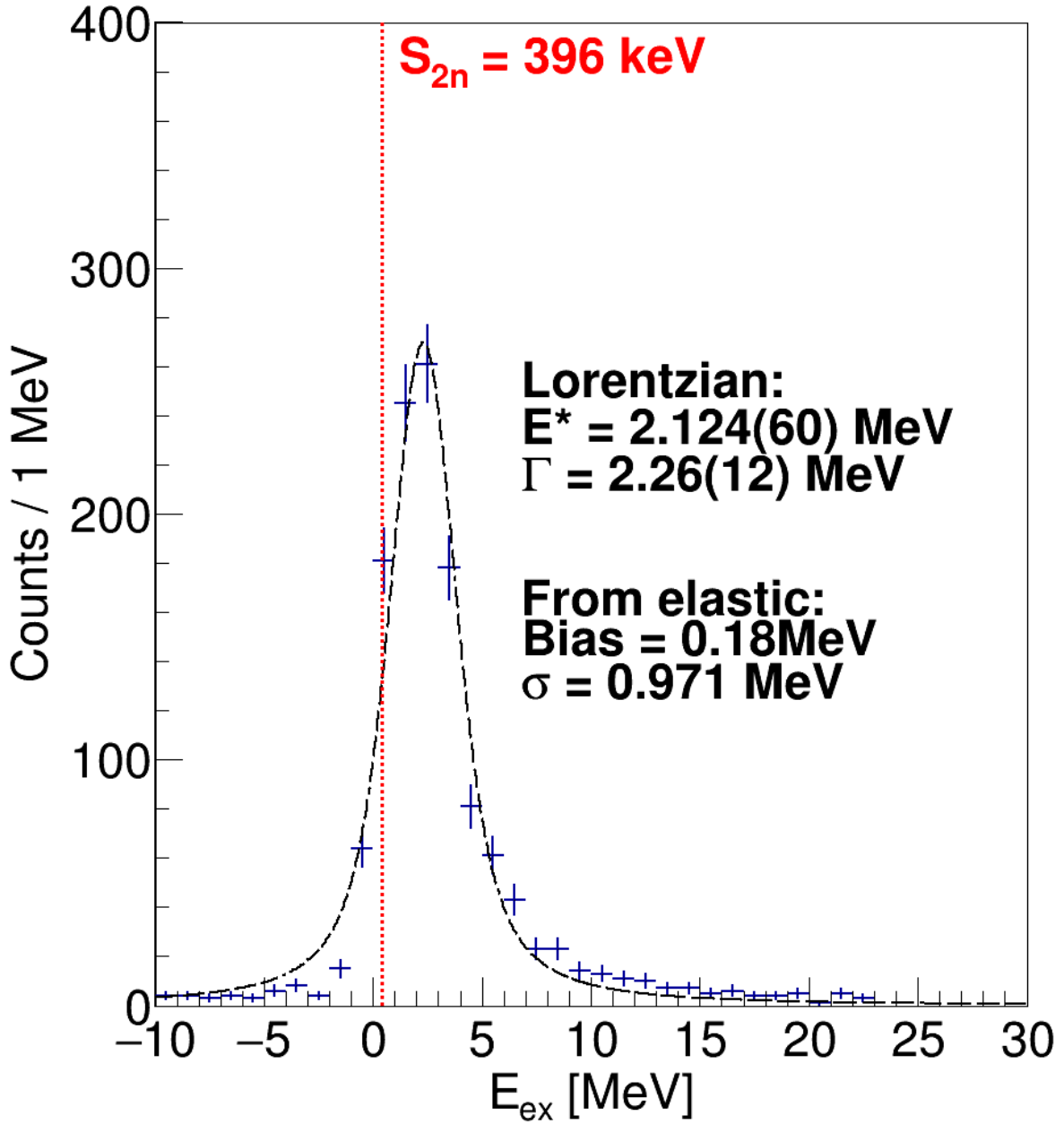




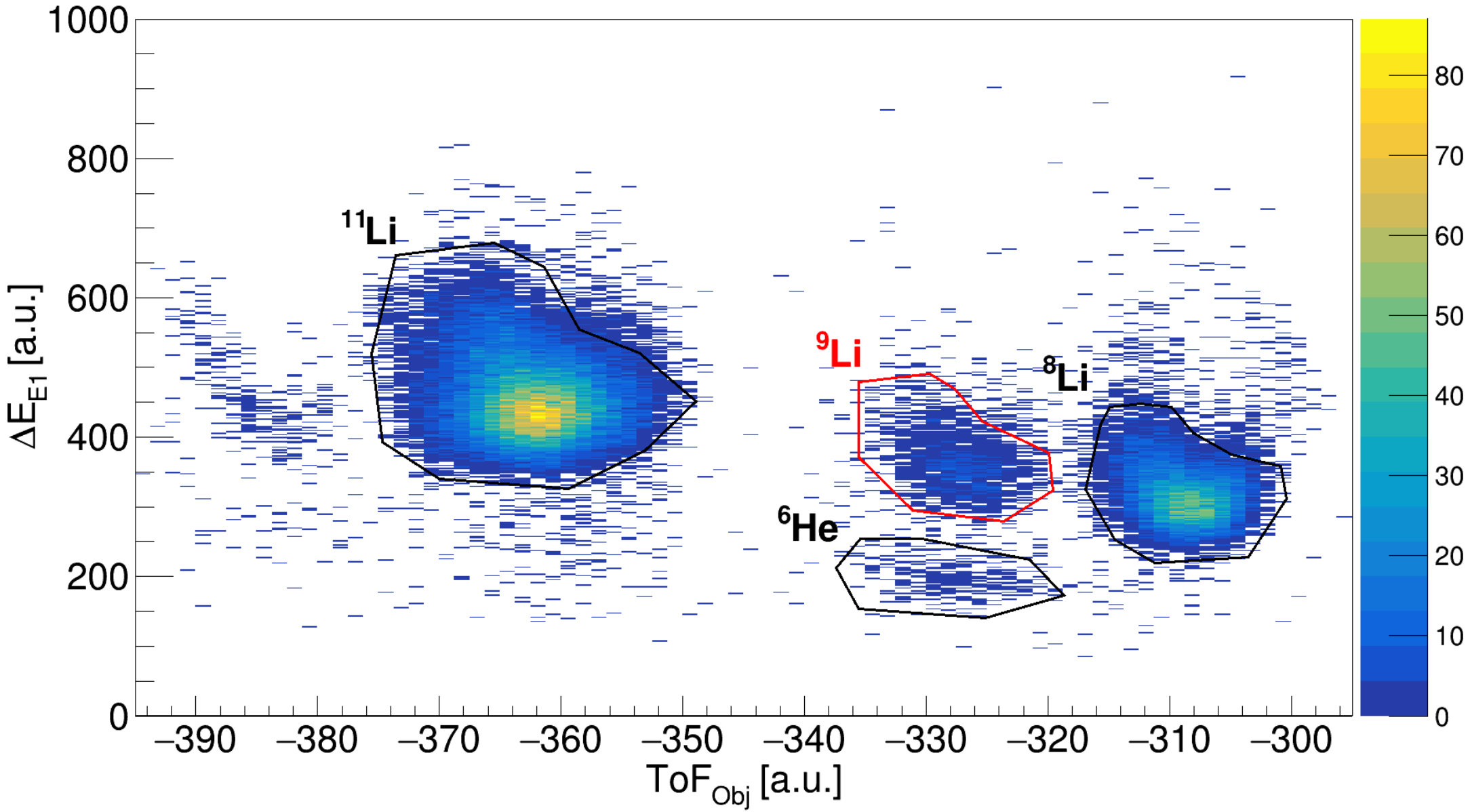
$^{11}Li + p \rightarrow {}^{9}Li + 2n + p'$

PRELIMINARY!



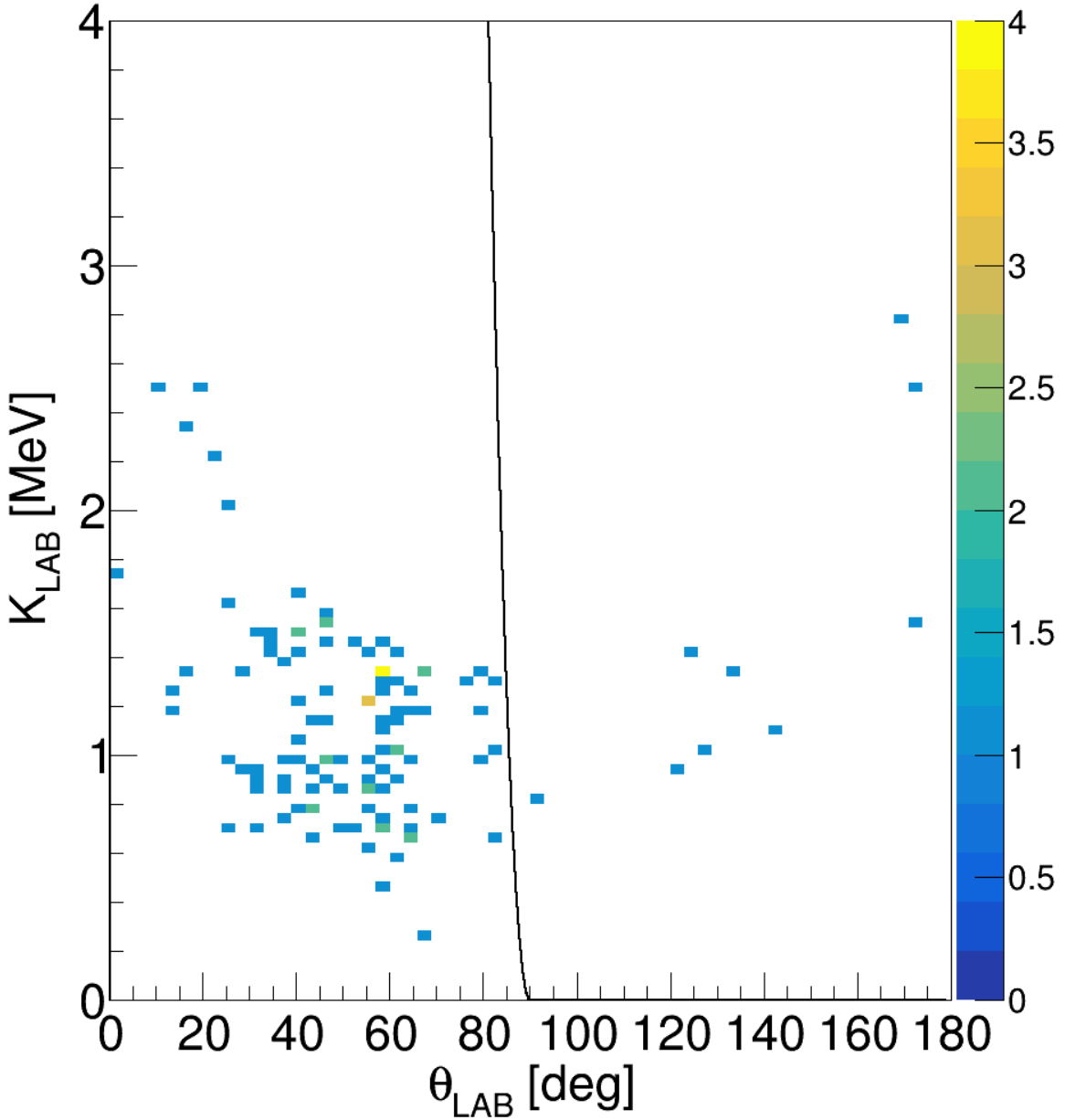


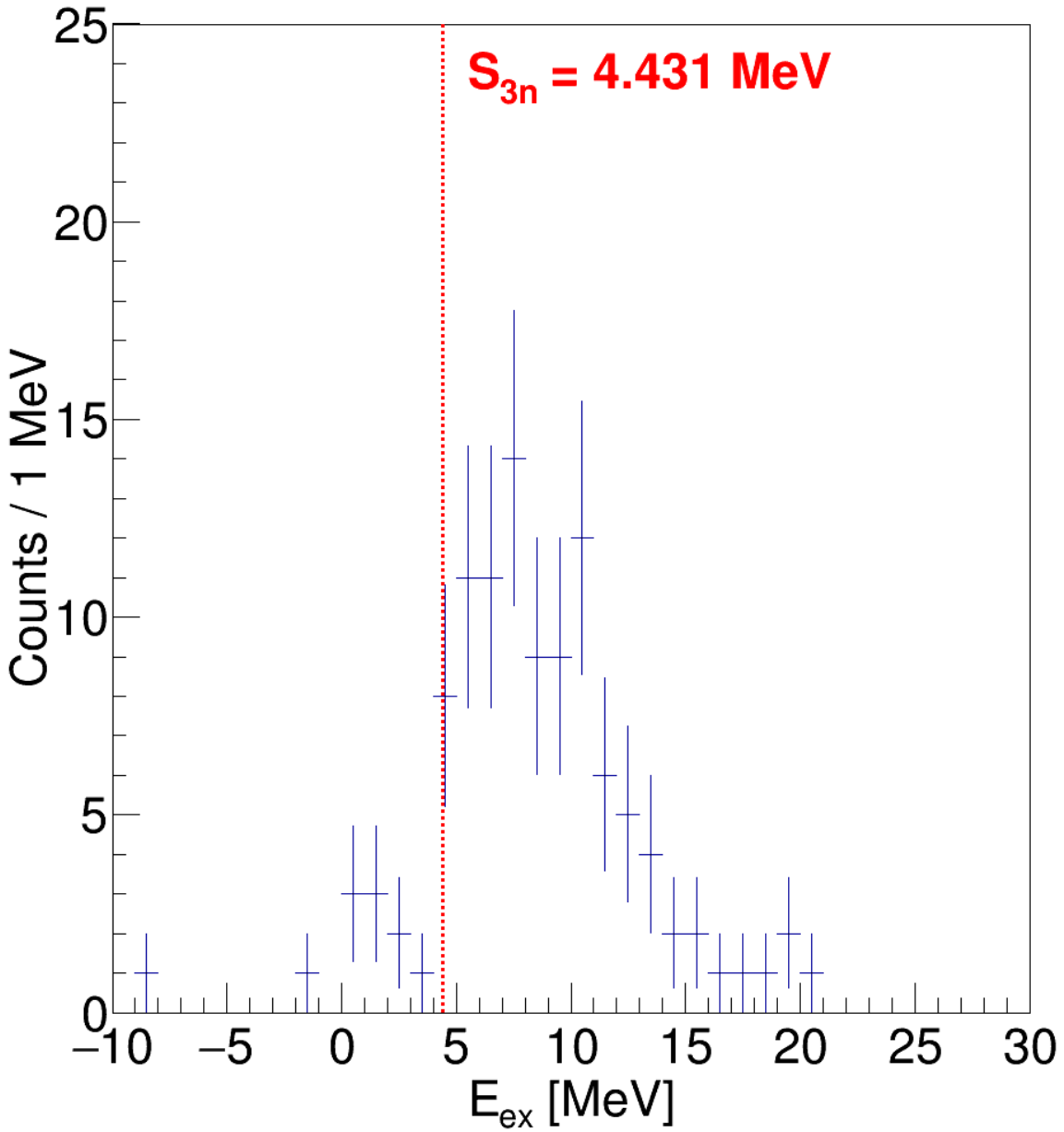
S800 centered on ^{8}Li with H_2@600Torr: Decay PID



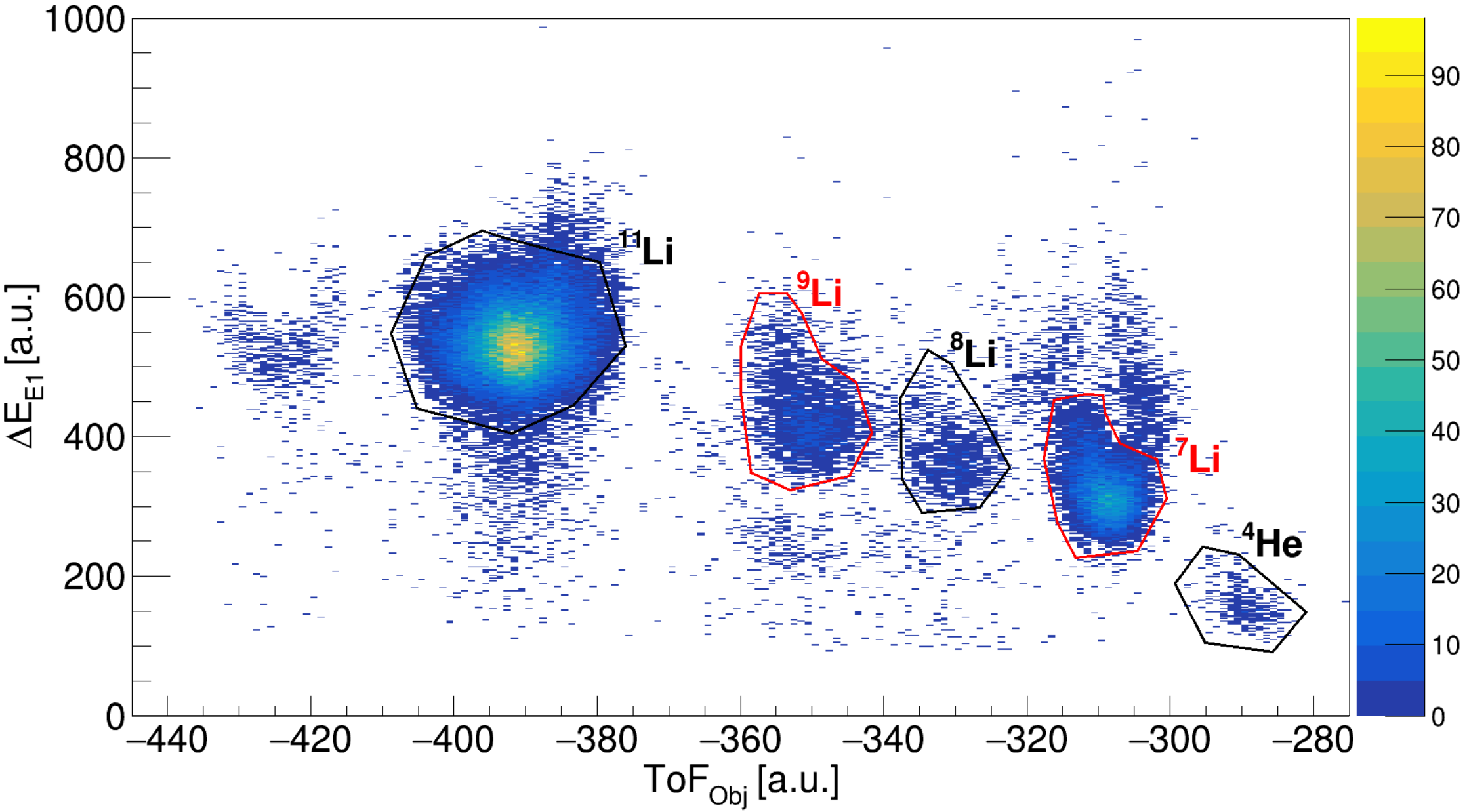
$^{11}Li + p \rightarrow {}^{8}Li + 3n + p'$

PRELIMINARY!



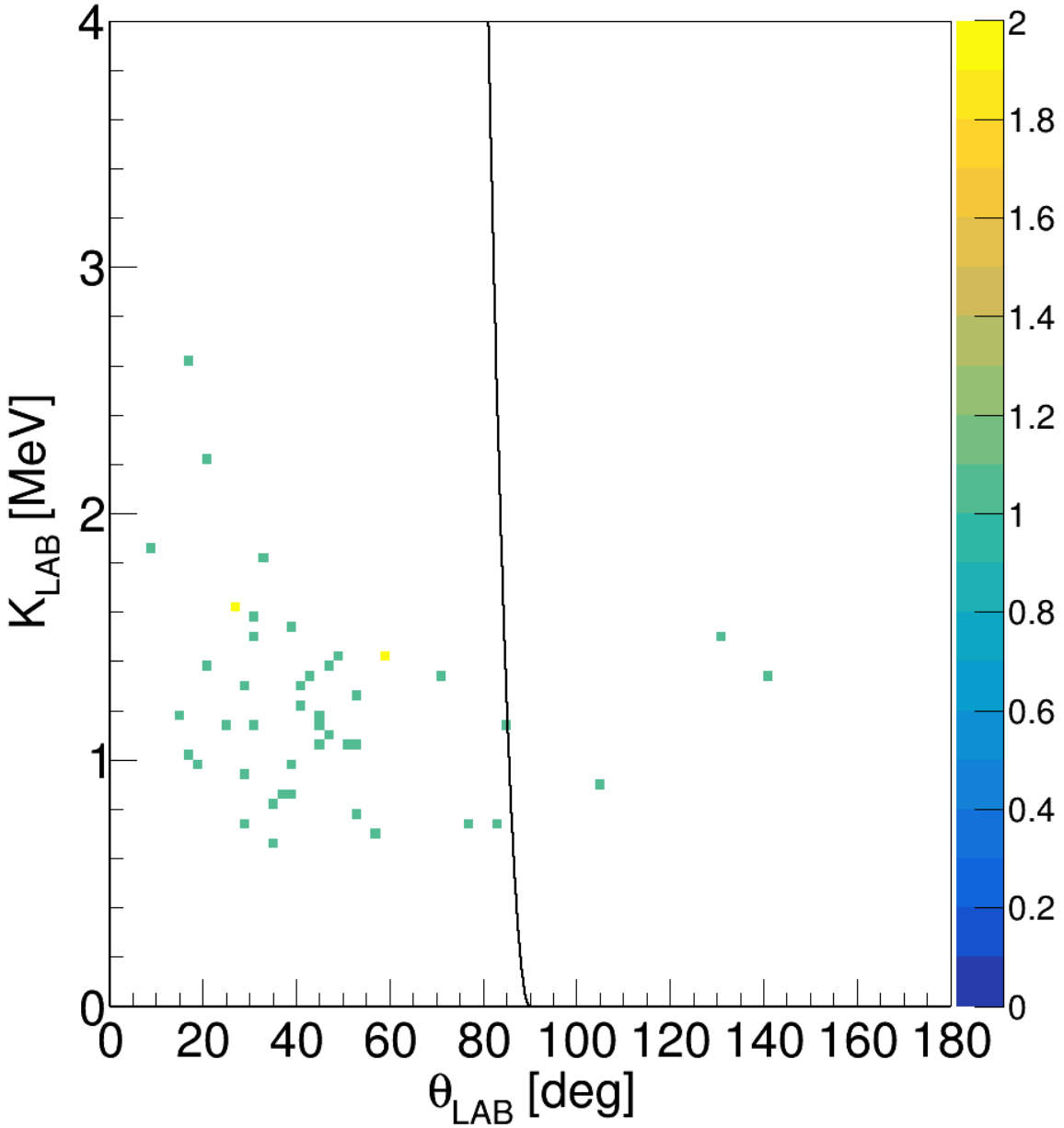


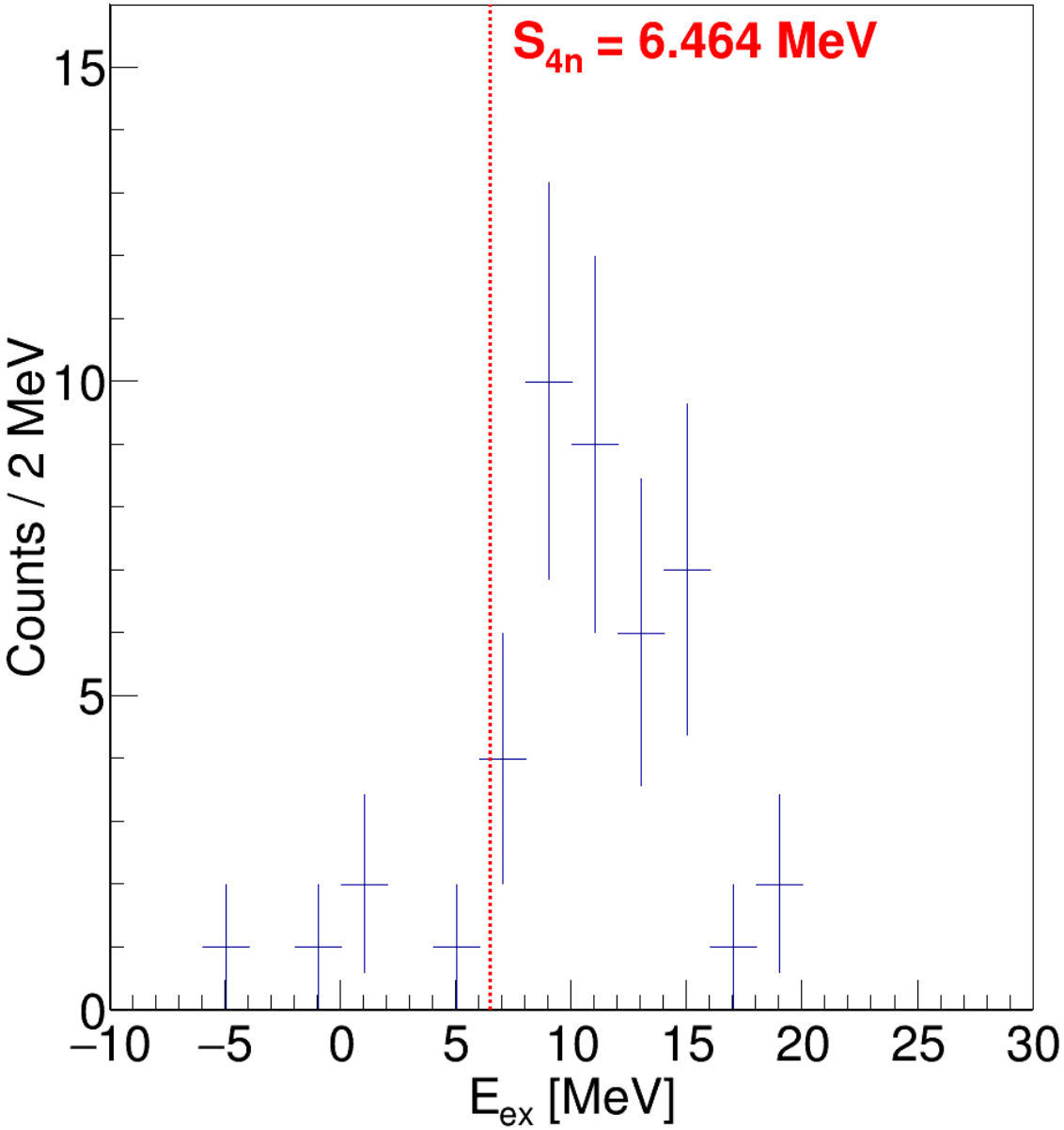
S800 centered on ^{7}Li with H_2@600Torr: Decay PID



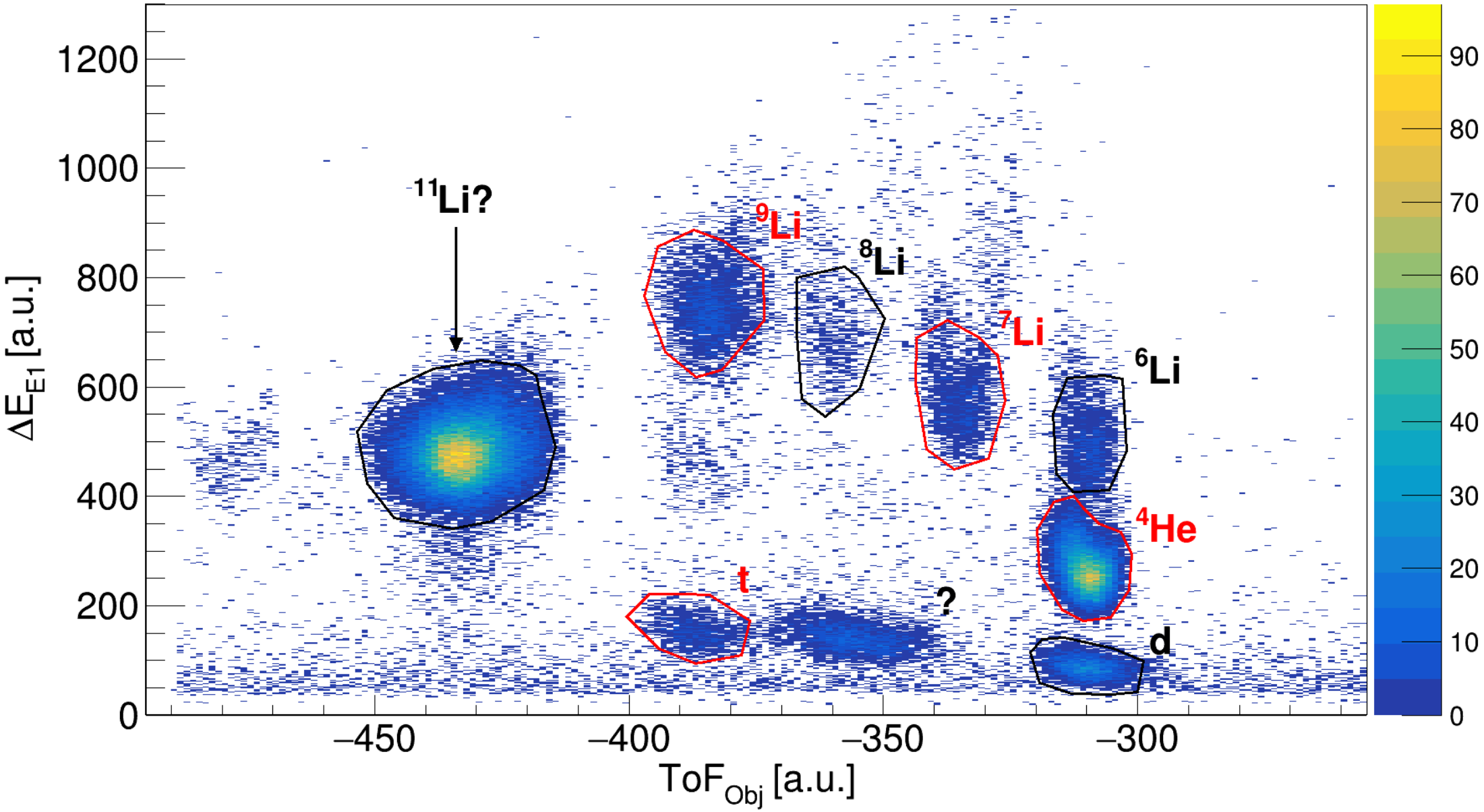
$^{11}Li + p \rightarrow {}^{7}Li + 4n + p'$

PRELIMINARY!



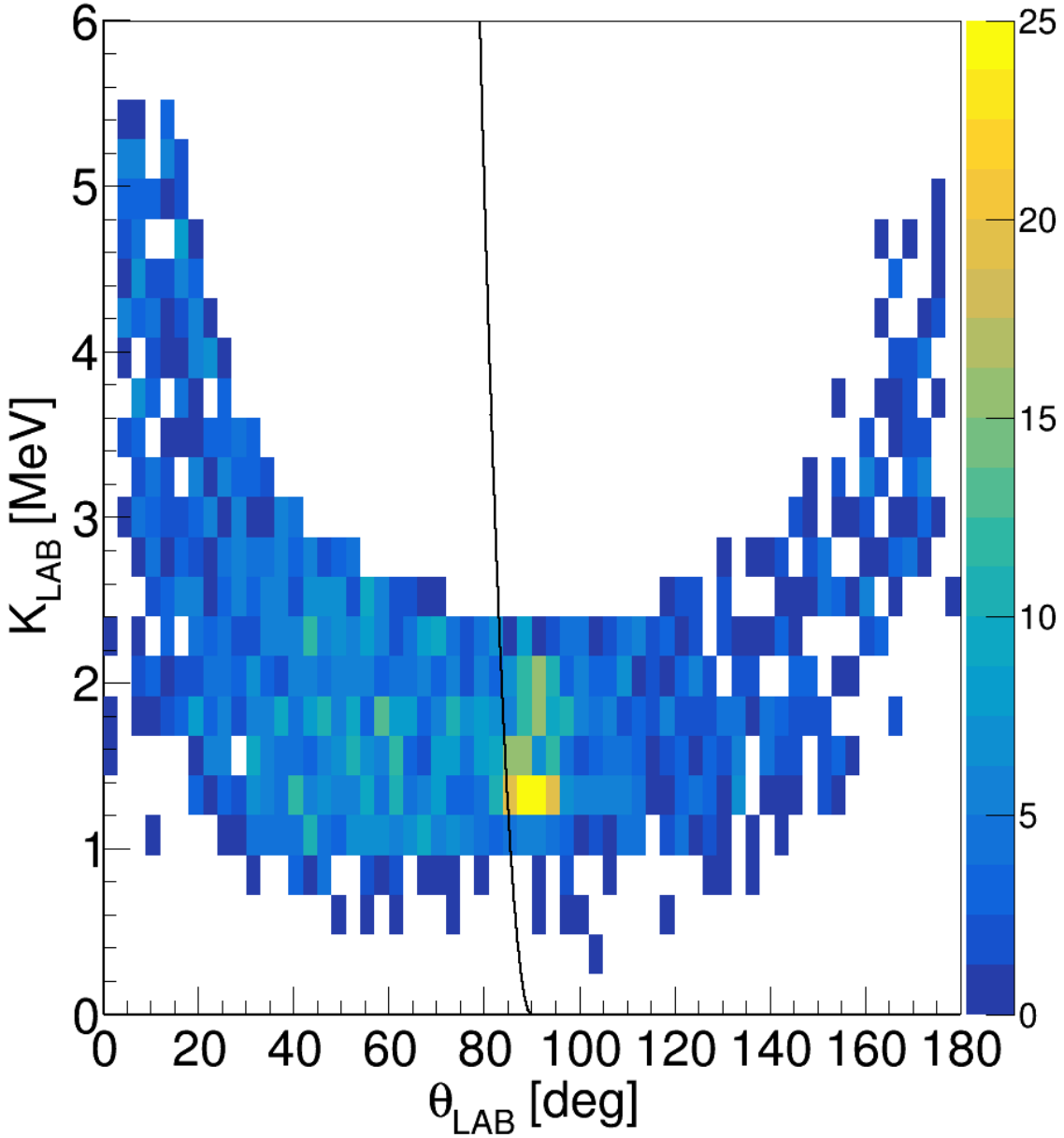


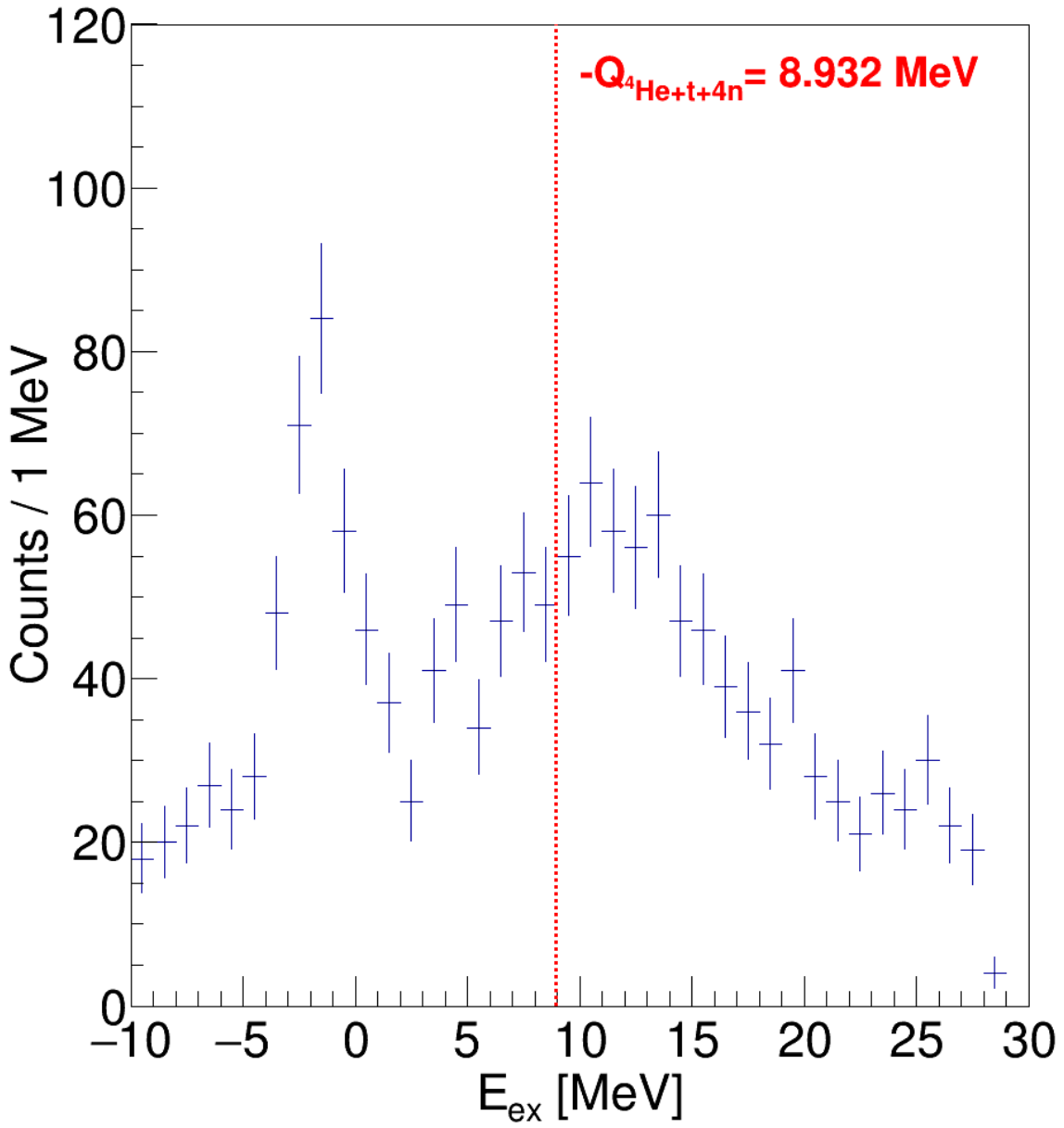
S800 centered on ^{4}He with H_2+CF_4@700Torr: Decay PID



$^{11}Li + p \rightarrow {}^{4}He + 4n + t + p'$

VERY PRELIMINARY!





Summary

- We measured the Pygmy dipole resonance of ^{11}Li at the very forward CM angles from 4º to 9º. We observe a resonance value of 2.124(60) MeV and a width of 2.26(12) MeV, significantly higher than previous measurements. The current fit does not take into account the nuclear penetrability, which will impact these values once considered.

- We also measured the decay channel to ^{8}Li, which could be interesting to study the structure of the ^{9}Li core of ^{11}Li. However, much more work is needed regarding this set of the data.

- A count excess in the decay channel to ^{4}He can be observed above the Q-value threshold, which could correspond to the IVGDR. However, much more work in this set of the data is needed before concluding anything.

Acknowledgements

J.M. López-González, Y. Ayyad, D. Bazin, J.C. Zamora, S.M. Ali, C. Ardelean, A. Barioni, F. Barranco, S. Beceiro-Novo, C. Benetti, C. Cabo, J. Chen, W. Dominik, M. Gai, U. Garg, S. Giraud, M.N. Harakeh, B.P. Kay, M. Kuich, J.A. Lay, C. Maher, G.W. McCann, A.J. Mitchell, W. Mittig, S. Noji, B. Olaizola, S. Painter, N.D. Pathirana, J. Pereira, G. Potel, Z. Rahman, D. Ramirez, Z. Serikow, D.K. Sharp, E. Vigezzi, B. Votaw, B. Wagner and R.G.T. Zegers

This material is based upon work supported by the U.S. Department of Energy, Office of Science, Office of Nuclear Physics, under Contract Number DE-AC02-06CH11357 (Argonne), and used resources of the Facility for Rare Isotope Beams (FRIB) Operations, which is a DOE Office of Science User Facility under Award Number DE-SC0023633. This work was also supported by the US National Science Foundation, grant nrs. PHY-2514797 and PHY-2310059. This work has also received financial support from the Xunta de Galicia (CIGUS Network of Research Centres) and the European Union through the Galicia Feder 2021-2027 Program. J. M. L. G. is supported by grant FPU24/03795 funded by the Ministery of Science, Innovation and Universities of Spain. Y. A. is supported by grant RYC2019-028438-I and PID2021-125995NA-I00 funded by MCIN/AEI/10.13039/501100011033 and by the Regional Government of Galicia under the program “Proyectos de excelencia” Grant No. ED431F2022/13. J. A. L. acknowledges grant No. PID2023-146401NB-I00 by MICIU/AEI/10.13039/501100011033 and by FEDER, UE. A. J. M. acknowledges the Australian Research Council Grant No. DP210101201 and the International Technology Center Pacific (ITC-PAC) under Contract No. FA520919PA138. B. O. acknowledges funding from the RYC2021-031494-I and PID2022-140162NB-I00 projects. S. B. N. acknowledges the grant RYC2020-030669 and PID2022-142557NA-I00 funded by MCIN/AEI/10.13039/501100011033, FSE+ and FEDER, UE And Grant ED431F 2024/01 funded by GAIN (Xunta de Galicia). J. C. was supported by the National Natural Science Foundation of China under Contracts No. 12475120 and No. 12435010.